UNIVERSITY of CALIFORNIA
SANTA CRUZ

NANOPARTICLE QUANTIZATION WITH A STRETCHABLE NANOPORE

A thesis submitted in partial satisfaction of the
requirements for the degree of

BACHELOR OF SCIENCE

in

APPLIED PHYSICS

by

Edolfo Garza-Licudine

10 June 2010

The thesis of Edolfo Garza-Licudine is approved by:

Professor William B. Dunbar
Advisor

Professor William B. Dunbar
Senior Theses Coordinator

Professor David P. Belanger
Chair, Department of Physics

Abstract

Nanoparticle Quantization With a Stretchable Nanopore

by

Edolfo Garza-Licudine

This paper demonstrates initial results with a portable device for nanoparticle detection and quantization, called the "qNano." The qNano instrument allows for detection of charged particles passing through a nanopore via electrophoresis. The instrument uses a stretchable plastic membrane with a pore on the order of a few hundred nanometers. The pore has been produced by a mechanical puncture, and stretching of the membrane allows for some control of the nanopore's radius. A voltage applied across the pore induces and electrophoretic effect, and particles translocate through the nanopore. The particle translocation is quantized with an ionic current through the pore. We show pressure control can be used to increase the rates of capture and translocation. We demonstrate quantization of liposome and polystyrene particles ranging from 200-400 nm in size. Capture rate (translocation events per second) is shown to be linear with respect to applied pressure and membrane stretching distance. Additionally, translocation event amplitude is shown to decrease with increasing pressure, but remains invariant to changes in the membrane stretching distance.

Contents

List of Figures **iv**

List of Tables **v**

Dedication **vi**

Acknowledgements **vii**

1 Introduction **1**

2 Methods **4**
2.1 Experimental Procedure 4
2.2 Polystyrene (220 nm, 400 nm) Experimental Conditions 4
2.3 Liposome Sample Preparation (200 nm) and Experimental Conditions 5
2.4 Data Analysis 5
2.5 Modeling 6

3 Results and Discussion **9**

4 Conclusions and Future Work **14**

5 Other Notes **15**

Bibliography **16**

List of Figures

1.1 Photograph of the qNano instrument. A USB connection provides electronic control from, and data logging to, a laptop or PC. The side knob provides mechanical control of the membrane stretching distance by adjusting the width of the jaws. 1

2.1 Example distribution of open-channel times. Open-channel time is defined as the amount of time the nanopore spends between any two successive particle translocations. Here the times have been sorted by length. 8
2.2 Example distribution of open-channel times after linearization. The probability of the open-chanel time has been run through the natural logarithm and replotted. As mentioned above, an r^2 value is used to test for goodness of fit. Most data has an r^2 value of .98 or above, indicating that 98% of data agrees with the model. 8

3.1 Example measured current (top, blue) with baseline drift, and total mean subtracted out. Spikes are 400 nm particle translocation events. The high-passed signal (bottom, red) has a stable baseline at 0 nA, but recorded events are visibly distorted - strictly downward current spikes in top signal become predominantly downward spikes in the high-pass signal (red), but with brief transient upward spikes after the event. 9
3.2 Typical translocation events. The top graph corresponds to a 400nm Polystyrene particle, the center graph is a 220nm Polystyrene particle, and the bottom graph is a 200nm Liposome particle. 10
3.3 Capture rate and amplitude for liposomes. Translocation rates (events per second) were found to be 2.8, 3.0, 4.2, and 6.1 for jaw widths of 54.02mm, 54.20mm, 54.40mm, and 54.80mm, respectively. 11
3.4 Translocation rate for 400nm Polystyrene particles. Translocation rates (events per second) were found to be 3.1, 17.7, 38.7, and 51.1 for pressures of 0kPa, 0.6kPa, 1.2kPa, and 1.8kPa, respectively. 12
3.5 Translocation amplitudes for 220nm and 400nm Polystyrene particles. Amplitudes are taken relative to baseline noise. Mean amplitudes for 220nm particles are 0.33 nA, 0.22 nA, and 0.16 nA at 0kPa, .6kPa, and 1.2kPa, respectively. Mean amplitudes for 400nm particles are 2.16 nA, 1.58 nA, 1.22 nA, and 1.03 nA at 0kPa, 0.6kPa, 1.2kPa, and 1.8kPa, respectively. Thus, amplitudes drop with increasing pressure, and 220nm particle amplitudes are much smaller ($\sim$10%) than the 400nm particle amplitudes. 13

List of Tables

3.1 Summary of capture rates for all particles. 12

To my parents, who have been everything a person could want.

Acknowledgements

Thanks to my advisor Bill, whose undying guidance and support has been instumental in allowing me to succeed. Thanks to Professor David Deamer for preparing biological samples and always having eye on the big picture. A special thanks to Dr. Sam Yu of Izon for his assistance in the pressure studies. Finally, thanks to undergraduates Darrel Deo, Asma Uz-Zaman, Alejandro Ayon, Thomas Schmitz, and Jessie Rucker for helping lay the groundwork and putting up with the tasks I found to be more unpleasant.

1 Introduction

Portable instruments allowing for real-time quantization of biological substances are needed for a wide range of scientific and industrial applications, including medicine, environmental monitoring, food monitoring, and drug screening [1]. Current nanoparticle-counting devices can be large enough to be rendered un-portable, and provide particle counting and size distribution quantization for in the range of 15-2500 μm [2]. There are very few portable instruments that can detect, count and identify nanometer-sized particles. We present our initial results with a resizable nanopore instrument called the "qNano" (Fig. 1.1), and demonstrate detection and quantization of liposome and polystyrene particles ranging from 200-400 nm. Potential applications include liposome distribution in pharmaceuticals, milk products, and plasma lipoproteins in hyperlipemic patients. The

Figure 1.1: Photograph of the qNano instrument. A USB connection provides electronic control from, and data logging to, a laptop or PC. The side knob provides mechanical control of the membrane stretching distance by adjusting the width of the jaws.

10-200 nm size range is also relevant for virus particle detection. Smallpox, for example, is a brick shaped DNA virus 200 nm in diameter, and has a $\sim$30% mortality rate [1].

Methods for nanoparticle detection are typically categorized as being label-based or label-

free [1]. For example, a compact multi-analyte surface plasmon resonance biosensor is described in [3]. In this method, small (< 30 nm) viruses such as the Norwalk virus can be detected. The method is label-based, and requires coating a channel's surface with an antibody for each respective virus to be quantified. Label-free methods typically involve optical methods or employ mass sensitive acoustic wave devices [1]. Clearly label-free methods offer a more generalized platform that allows for greater flexibility for a given application.

The qNano instrument uses this label-free method of quantization, allowing for a wide range of particles to be tested. Additionally, varying the pore width allows for greater flexibility with regards to filtering out particles above a given size. Nanopores are an established method for studying biophysics at the single-molecule level, and offer great promise for inexpensive genomic sequencing [4]. The qNano instrument uses a thermoplastic polyurethane membrane with a nanometer-scale pore that has been produced by puncturing the membrane with a metallic needle. The membrane is hooked into the jaws of the device, and can be stretched by moving the jaws away from one another. This allows for real-time control of the nanopore's radius.

The qNano uses an integrated patch-clamp amplifier, a device for which Neher and Sakmann received the Nobel prize in "Physiology or Medicine" in 1991 [7]. Voltage applied across the membrane is used to drive the electrophoretic flow, and ionic current through the nanopore channel can then be measured. Translocating particles produce quantifiable steps or spikes in the ionic current, and the transient blockade can provide information about each translocating particle. In the current device, the geometry of each pore is unknown. The latest version of the instrument allows one to use pressure as an additional driving force for pushing molecules through the detection channel at increasing rates.

It is interesting to note the strength of the electric field within the nanopore itself can be quite large for relatively small applied voltages. Recall the electric field can be expressed in terms of electric potential and distance

$$\vec{E} = \frac{v}{m}$$

For a nanopore of sufficiently small depth, even an applied voltage of .1v can easily create an electric field within the pore whose magnitude is a thousand times stronger than the original applied field. Such fields almost guarantee charged particle translocation will occur, if the particle is close enough to the opening of the pore.

Wilmott [5] has shown the thermoplastic nanopore's geometry to be conical in shape, and the radius can be reversibly deformed over an order of magnitude by stretching and relaxing the membrane. Additionally, Sowersby [6] has shown the device can generally be used as a tunable molecular sensor, and more specifically as a device to detect and control the gating of DNA molecules. We present our approach with our initial experiments and analysis of particle translocations, quantifying capture rate and blockade event amplitude trends as a function of pressure and nanopore membrane stretching width. In particular, we examine these patterns for liposome and polystyrene particles ranging from 200-400 nm.

2 Methods

2.1 Experimental Procedure

Fluid cells are washed with de-ionized water, then dried with a clean cloth. Once the lower fluid cell was in place, 50μL of buffer solution is placed into the center channel, with care taken to ensure no bubbles were introduced. The membrane was primed with a drop of buffer on both the sides of the nanopore, then set onto the jaws to remain in place. The upper fliud cell was the set into place, and 50μL of buffer were added to the upper fluid cell. Pore width was controlled by adjusting the jaw width, pressure was controlled with an external pump connected to the upper fluid cell (not shown in Figure 1.1), and voltage was controlled by the connected computer. At constant voltage (typically 0.2 V), the pore was known to be open when a direct correlation (1 to 1 mapping) could be observed between ionic current and adjustment of jaw width - once this was achieved, particles were added into the upper fluid cell. A Faraday cage surrounds the entire fluid cell to allow to reduce noise to $\sim$2-5 pA RMS.

2.2 Polystyrene (220 nm, 400 nm) Experimental Conditions

All experiments used a voltage of 0.2 V. The standard electrolyte for experiments in this paper consists of 0.1 M aqueous KCl, buffered using 0.01 M tris(hydroxymethyl)aminomethane (Tris, pH 8). Added are 0.01% of Triton X-100 (to aid wetting of the pore) and 3 mM EDTA. The nanopore and cell were cleaned with standard buffer and the cell reloaded with sample between runs. Particle

suspensions were made by diluting a stock solution of particles in standard electrolyte. These particles were diluted in the standard electrolyte and were ultrasonicated for at least 5 minutes prior to use. Carboxylated polystyrene particles with nominal average sizes of 400 nm and 220 nm (Thermo Scientific) were received at concentrations of 2.8×10^{11} and 1.7×10^{12} particles/mL, respectively.

2.3 Liposome Sample Preparation (200 nm) and Experimental Conditions

Lipid vesicles (liposomes) were prepared by a standard extrusion technique. Briefly, 1-palmitoyl 2-oleoylphosphatidic acid (POPA, Avanti Polar Lipids) was used in order to assure uniform negative charge on the membrane surfaces. The dry lipid was dispersed by vortexing in 1.0 ml of the IZON buffer at a concentration of 1.0 mg/ml, then extruded ten times through a 200 nm polycarbonate filter in the Avanti syringe extrusion device. This method produces single-layered liposomes in a size range close to the diameter of the filter pores. We estimate 3×10^{13} vesicles per ml of liposomes containing 5 mg lipid per ml. Liposome experiments used a voltage of 0.2 V, and a buffer to liposome ratio of 10:1.

2.4 Data Analysis

All analysis was done in Matlab R2007b. Because the measured current (filtered at 5 kHz and sampled at 50 kHz) has a tendency to drift, a 50Hz high-pass unity gain Butterworth filter was employed to remove DC content and low-frequency drift. Specifically, we used a 1Hz stopband frequency (80dB attenuation) with a 50Hz passband frequency (1dB ripple). The z-form transfer function for our filter is

$$H(z) = \frac{.9973 - 2.9919z^{-1} + 2.9919z^{-2} - .9973z^{-3}}{1 - 2.9946z^{-1} + 2.9892z^{-2} - .9946z^{-3}}$$

The filter had a tendency to distorted longer-lasting events, so we used the high-pass signal for an efficient global search for candidate events, using a threshold (e.g., > 3 times the RMS noise). Indices in the sampled current below this threshold are next used as the warm-start within the originally recorded signal. The original data tended to have a fairly consistent baseline locally, that is, the current drift is negligible for a small enough subsection of data. We obtain a relative amplitude A_{rel} for each translocation event, defined as

$$A_{\text{rel}} := \mu_{\text{local}} - A_{\text{min}}$$

with μ_{local} defined as the average of the current 300 samples before the start of each candidate event, and A_{min} defined as the minimum value of the current within the candidate event. A candidate event was counted and A_{rel} quantified if the blockade A_{min} was lower than a threshold equal to μ_{local} minus 5 times the RMS noise.

2.5 Modeling

Because particle translocations partially block the nanopore and lead to a measurable drop in current, we naturally come to the idea of open channel time. We define open channel time as the time between any two particle translocations - equivalently, this is the time the nanopore spends without particle translocations. Particle translocation times are identified as the time at which A_{min} occurs for quantified events. Although time between events neglects the duration of events, such durations were observed to be negligible compared to inter-event times. We model each individual open channel time as independent random events. This leads us to an exponentially-distributed collection of open channel times, obeying the following probability density function

$$p(t) = \begin{cases} \lambda e^{-\lambda t} & t \geq 0 \\ 0 & t < 0 \end{cases}$$

where λ is the Poisson rate, here taken to be the translocation (or capture) rate. Taking the natural logarithm of this density function for $t \geq 0$, we obtain the following linear equation

$$\ln(p(t)) = \ln(t) - \lambda t \tag{2.1}$$

Using Matlab R2007b, we used the built-in functions `polyfit` and `polyval` to obtain a linear best fit and a sequence of best fit values. We can then test for deviation from this model (2.1) by use of an r^2 value, defined as such

$$r^2 := 1 - \left\{ \sum_i^n (y_i - \bar{y_i})^2 \right\} \Big/ \left\{ \sum_i^n (y_i - \mu)^2 \right\}$$

with the following variable definitions

$$\begin{aligned} y_i &:= i\text{th data point} \\ \bar{y_i} &= \text{Best-fit value at the } i\text{th data point.} \\ \mu &= \text{The experimentally-obtained mean} \end{aligned}$$

This is the ratio of the sum of squares of the regression to the total sum of squares, and is restricted between 0 and 1, where a value of 1 is taken to be a perfect fit. Outliers were dealt with by using the best 98% of data for computation.

To convince the reader that capture rate truly is exponentially distributed, we present Figs. 2.1 and 2.2 as an example of data from a typical experiment. The first Fig. shows what quite clearly appears to be an exponential distribution, but is not yet quantified as such. The second Fig. shows a logarithmic scaling and fitting to a straight line - empirical proof of the corectness of our models.

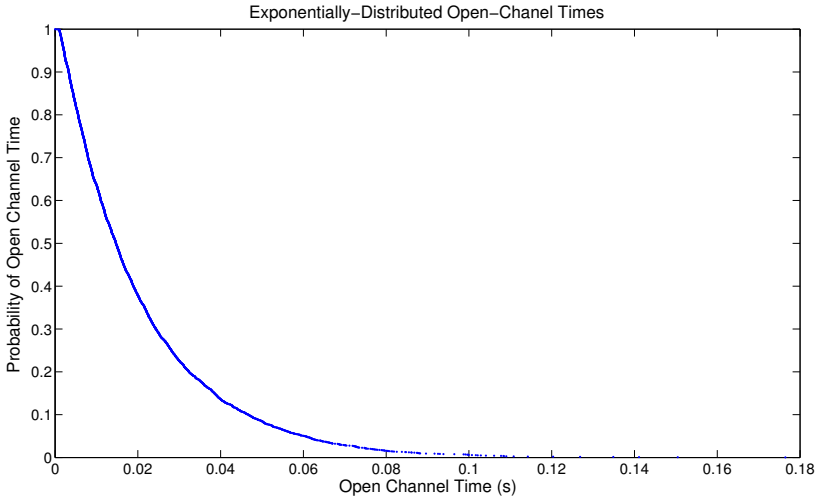

Figure 2.1: Example distribution of open-channel times. Open-channel time is defined as the amount of time the nanopore spends between any two successive particle translocations. Here the times have been sorted by length.

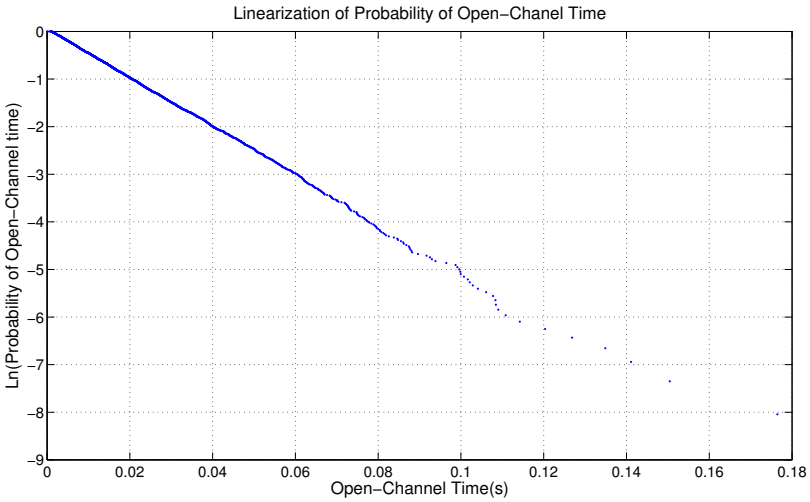

Figure 2.2: Example distribution of open-channel times after linearization. The probability of the open-chanel time has been run through the natural logarithm and replotted. As mentioned above, an r^2 value is used to test for goodness of fit. Most data has an r^2 value of .98 or above, indicating that 98% of data agrees with the model.

3 Results and Discussion

We begin with examples of typical signals seen in different experiments.

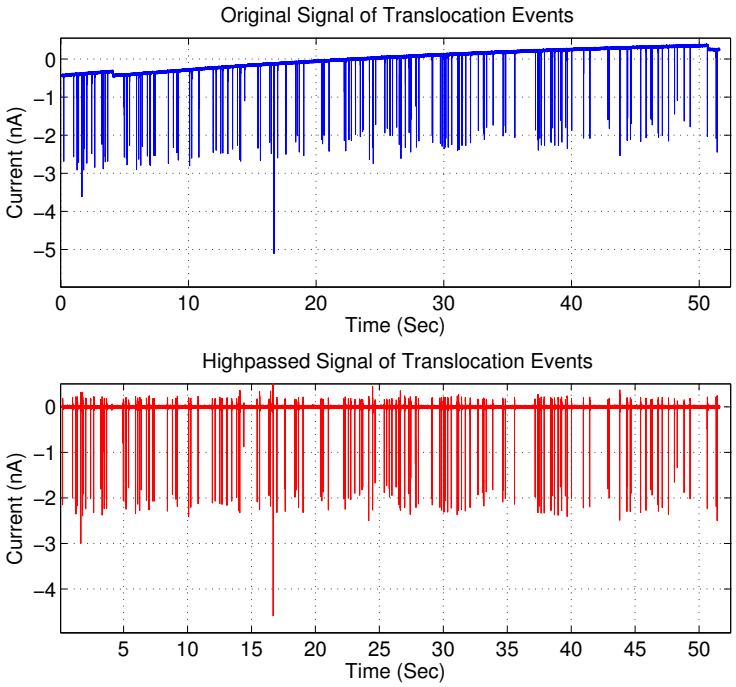

Figure 3.1: Example measured current (top, blue) with baseline drift, and total mean subtracted out. Spikes are 400 nm particle translocation events. The high-passed signal (bottom, red) has a stable baseline at 0 nA, but recorded events are visibly distorted - strictly downward current spikes in top signal become predominantly downward spikes in the high-pass signal (red), but with brief transient upward spikes after the event.

Figure 3.1 is a typical time-history of translocating particles seen after an experiment has been run. Figure 3.2 is a typical real-time view of particle translocation during an experiment. Experiments typically generate hundreds to thousands of events, and characteristics such as open-

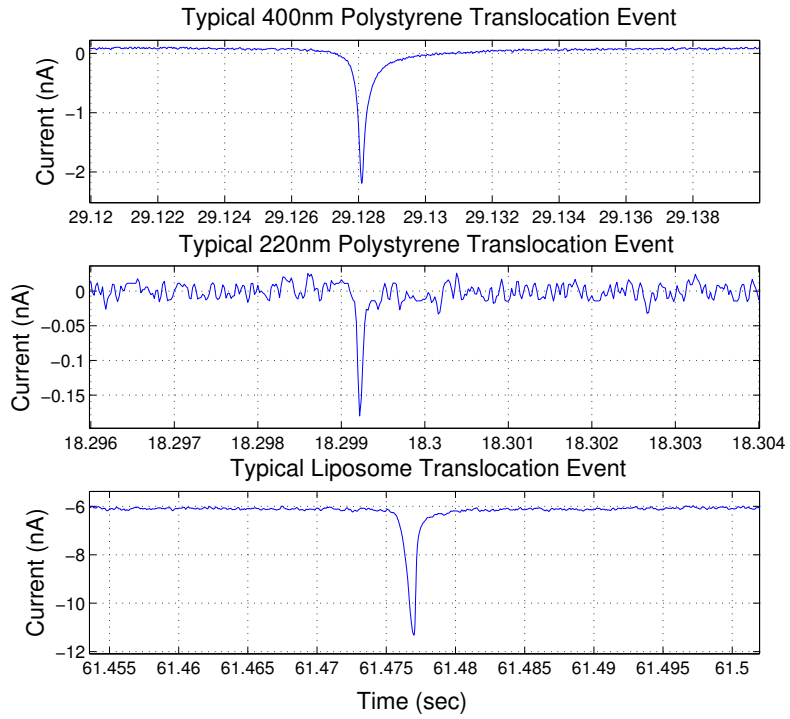

Figure 3.2: Typical translocation events. The top graph corresponds to a 400nm Polystyrene particle, the center graph is a 220nm Polystyrene particle, and the bottom graph is a 200nm Liposome particle.

channel time and amplitude are used as summary statistics.

We look next to the behavior of 200nm liposome particles as a function of increasing nanopore size. Because of the elasticity of the membrane, the exact width of the nanopore is unknown, and we instead measure the mechanical separation of the clamps used to hold the nanopore in place (hereafter termed the jaw width). As evidenced by Figure 3.3, capture rates appear to increase linearly with increasing jaw width while amplitude remains invariant.

The polystyrene particles were used in a pressure study and has been shown to influence both translocation rates and amplitude distributions, as seen in Figures 3.4 and 3.5. A summary of the translocation statistics can be found in Figure 3.1.

It is important to note that while the applied pressure was measured in increments of 0.6kPa, there already exists an induced pressure resulting from the upper fluid cell's positioning and the force due to gravity. We believe the decrease in amplitudes with increase in pressure is directly

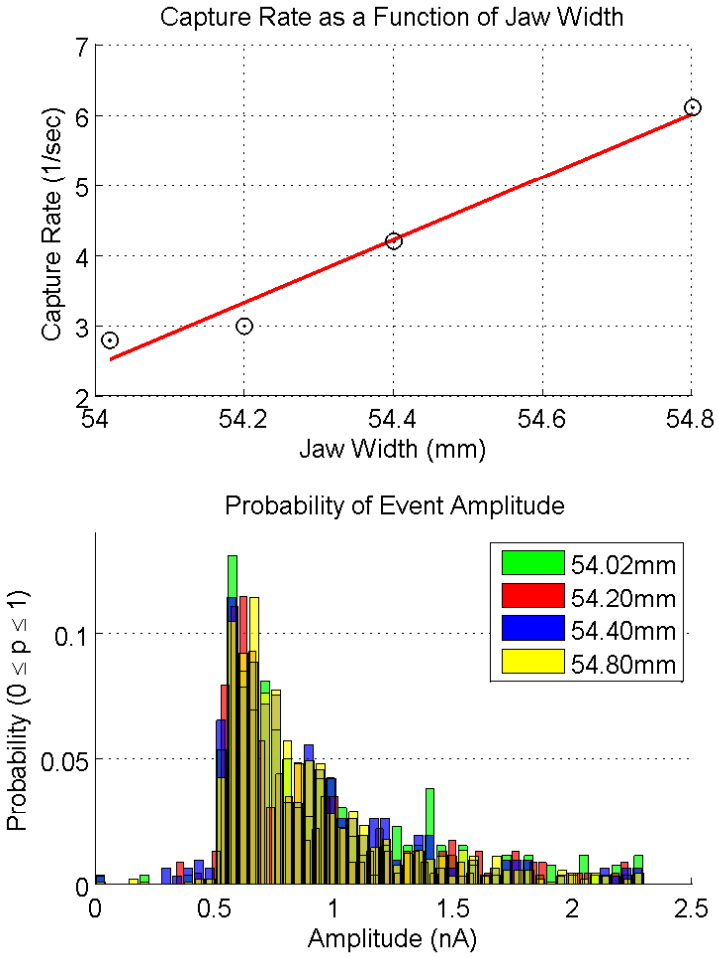

Figure 3.3: Capture rate and amplitude for liposomes. Translocation rates (events per second) were found to be 2.8, 3.0, 4.2, and 6.1 for jaw widths of 54.02mm, 54.20mm, 54.40mm, and 54.80mm, respectively.

related to the corresponding increase in translocation rates. At high enough translocation speeds, the instrument's sample rate and bandwidth play an increasingly restrictive role in seeing the entire event. Typical events at high pressures were observed to have an undersampling of data points at the minima of a given event.

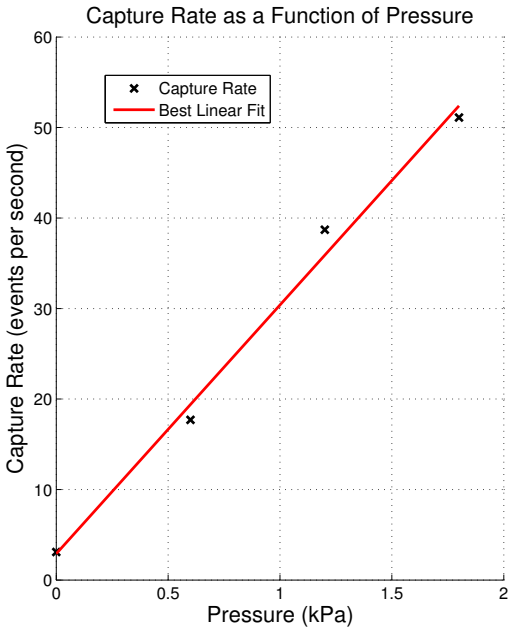

Figure 3.4: Translocation rate for 400nm Polystyrene particles. Translocation rates (events per second) were found to be 3.1, 17.7, 38.7, and 51.1 for pressures of 0kPa, 0.6kPa, 1.2kPa, and 1.8kPa, respectively.

Particle Type	Particle Size (nm)	Varying Parameter	Capture Rate (1/sec)
Liposome	200	54.02mm Jaw Width	2.8
Liposome	200	54.20mm Jaw Width	3
Liposome	200	54.40mm Jaw Width	4.2
Liposome	200	54.80mm Jaw Width	6.1
Polystyrene	400	0kPa	3.1
Polystyrene	400	0.6kPa	17.7
Polystyrene	400	1.2kPa	38.7
Polystyrene	400	1.8kPa	51.1

Table 3.1: Summary of capture rates for all particles.

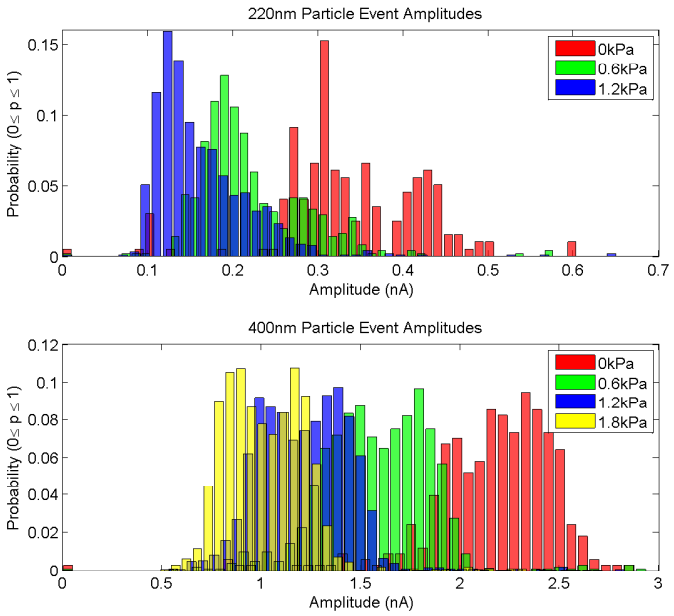

Figure 3.5: Translocation amplitudes for 220nm and 400nm Polystyrene particles. Amplitudes are taken relative to baseline noise. Mean amplitudes for 220nm particles are 0.33 nA, 0.22 nA, and 0.16 nA at 0kPa, .6kPa, and 1.2kPa, respectively. Mean amplitudes for 400nm particles are 2.16 nA, 1.58 nA, 1.22 nA, and 1.03 nA at 0kPa, 0.6kPa, 1.2kPa, and 1.8kPa, respectively. Thus, amplitudes drop with increasing pressure, and 220nm particle amplitudes are much smaller ($\sim$10%) than the 400nm particle amplitudes.

4 Conclusions and Future Work

Particle translocation rates increase linearly with increases in pressure and jaw width, while particle amplitudes remain invariant with changes in jaw width and decrease with increases in pressure. Future experiments include both changes in voltage and their relative difference to changes in pressure, and changes in dilution. Additionally, we aim to test for smaller particle sizes in the range of 50nm, as detection at this level leads into preliminary detection of virus particles of interest. We also plan to model pore dynamics as a narrowing cone with the corresponding differential system, in attempts to estimate the channel geometry as a function of changes in jaw width. Future analysis must consider surface charge affects along the pore boundary, and potential non-specific binding between particles and the pore at varying locations. For both label-based and label free methods of nanoparticle detection, a principal limiting factor to biosensor performance is non-specific binding [1].

5 Other Notes

It should be noted that this paper, with a few minor changes, has been accepted for publication at the 32nd Annual International Conference of the IEEE Engineering in Medicine and Biology Society [8].

Bibliography

[1] J. J. Gooding. Biosensor technology for detecting biological warfare agents: Recent progress and future trends. *Analytica Chimica Acta*, 559, pp. 137-51 (2006).

[2] Particle Technology Laboratories, Ltd. URL: `http://www.particletechlabs.com/`.

[3] T. M. Chinowsky, et al. Portable 24-analyte surface plasmon resonance instruments for rapid, versatile biodetection. *Biosensors and Bioelectronics*, 22, pp. 2268-75 (2007).

[4] D. Branton, et al. The potential and challenges of nanopore sequencing. *Nat Biot*, 26, pp. 1146-53 (2008).

[5] G.R. Willmott and P.W. Moore. Reversible mechanical actuation of elastomeric nanopores. *Nanotechnology*, 19, pp. 475-504 (2008).

[6] S.J. Sowerby, M.F. Broom, and G.B. Petersen. Dynamically resizable nanometre-scale apertures for molecular sensing. *Sensors and Actuators B*, 123, pp. 325-30 (2007).

[7] The Nobel Prize in Physiology or Medicine 1991 URL: `http://nobelprize.org/nobel_prizes/medicine/laureates/1991/`.

[8] E. Garza-Licudine, D. Deo, S. Yu, A. Uz-Zaman, D. Deamer, W.B. Dunbar Portable Nanoparticle Quantization Using a Resizable Nanopore Instrument - The IZON qNano. *32nd Annual EMBS Conference.* Accepted for publication September 2010.